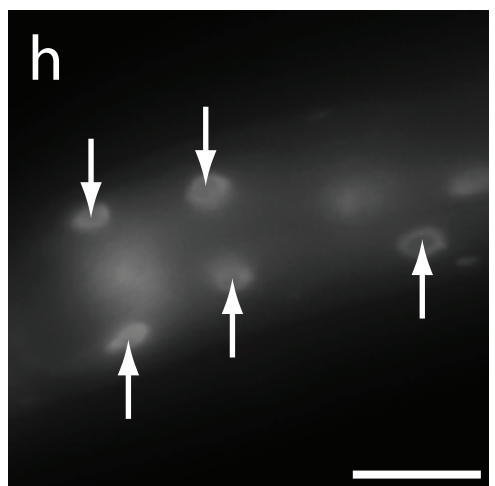
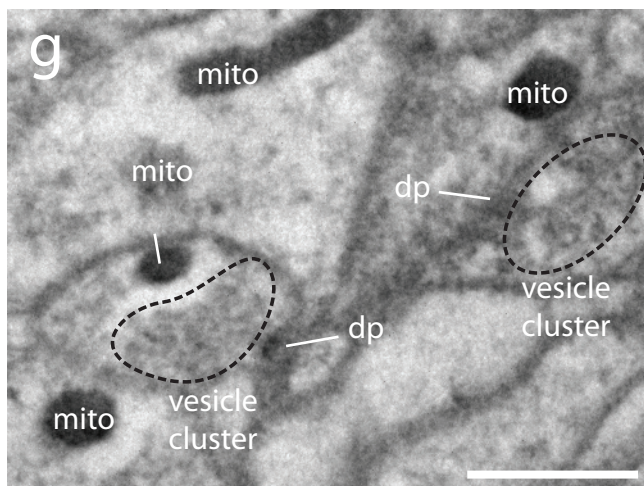
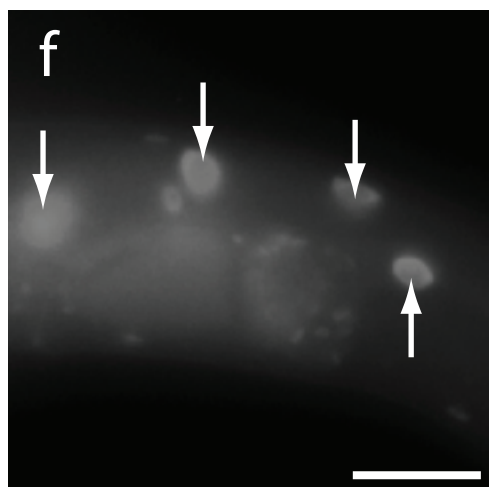
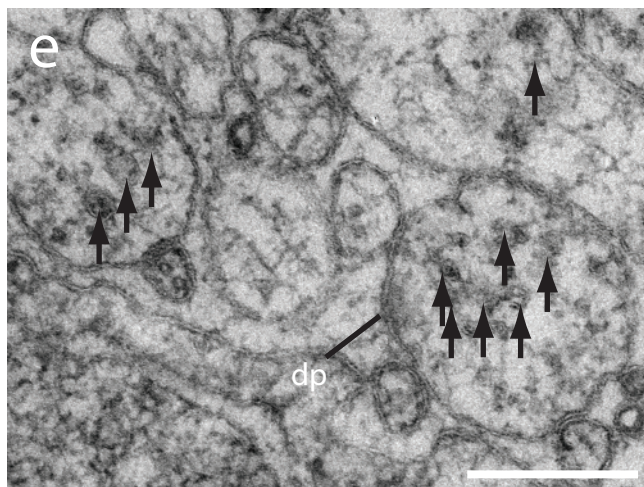
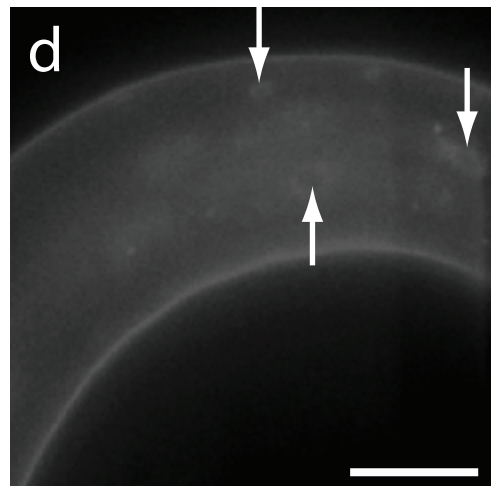
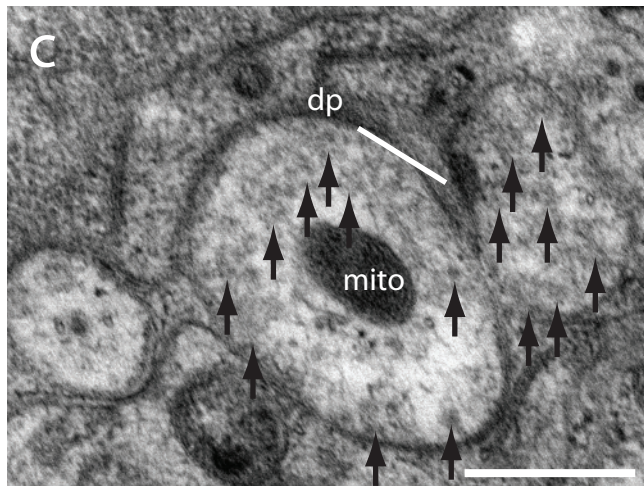
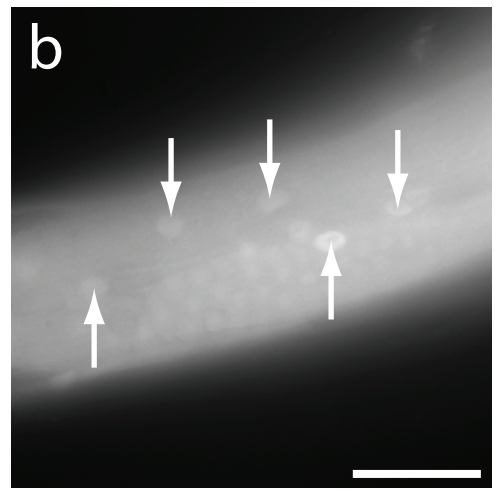
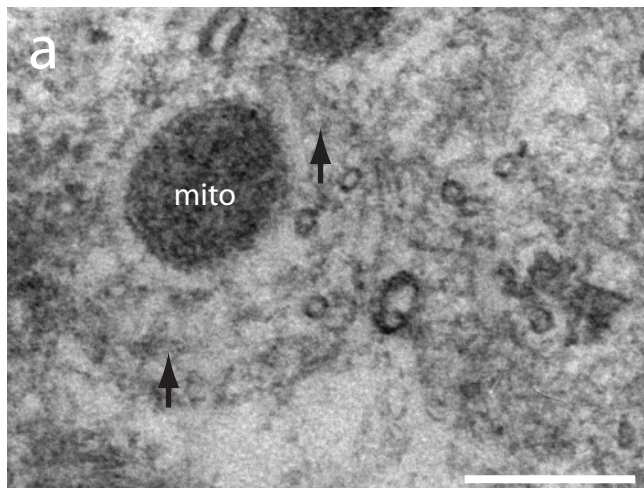
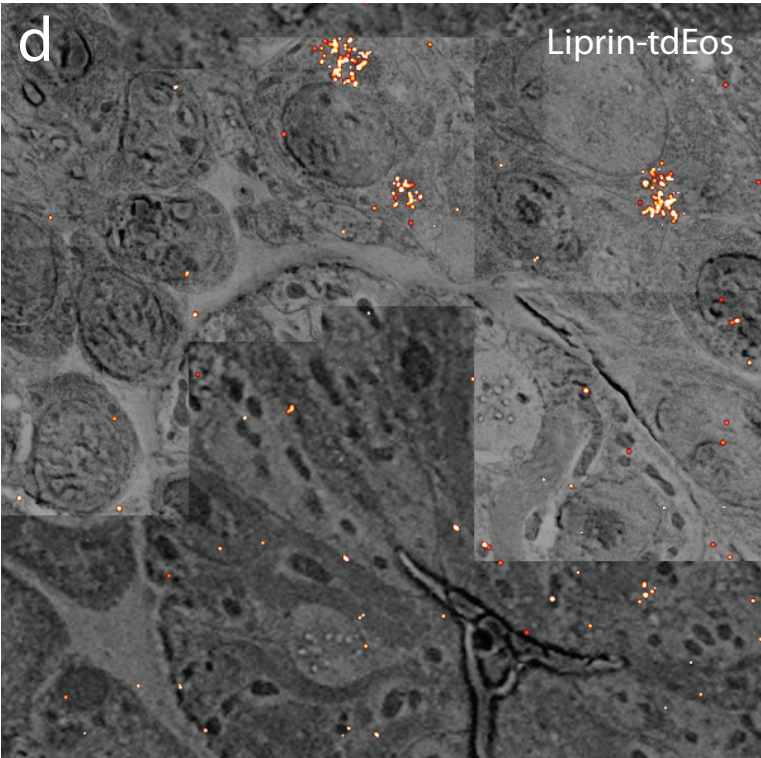
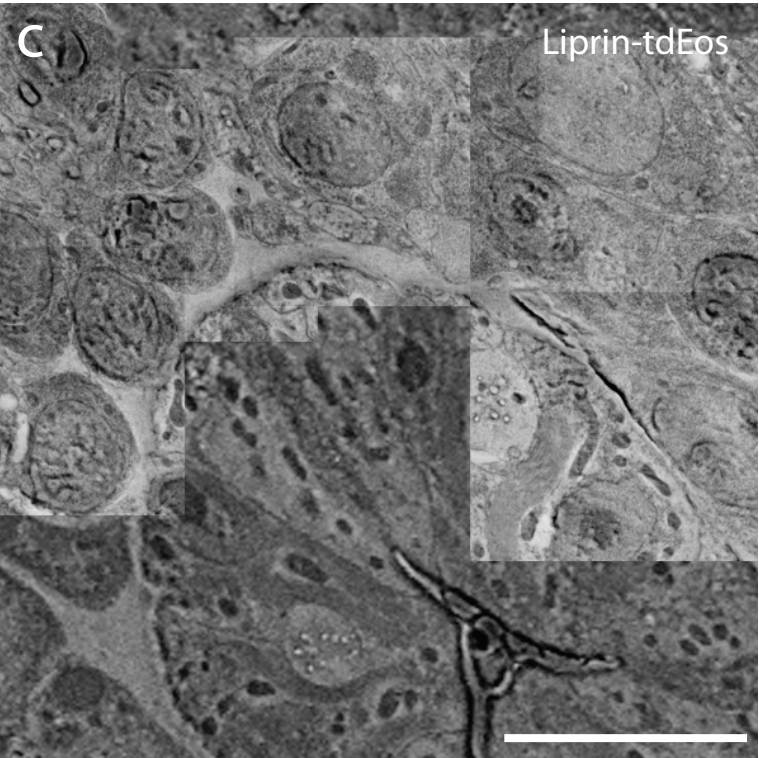
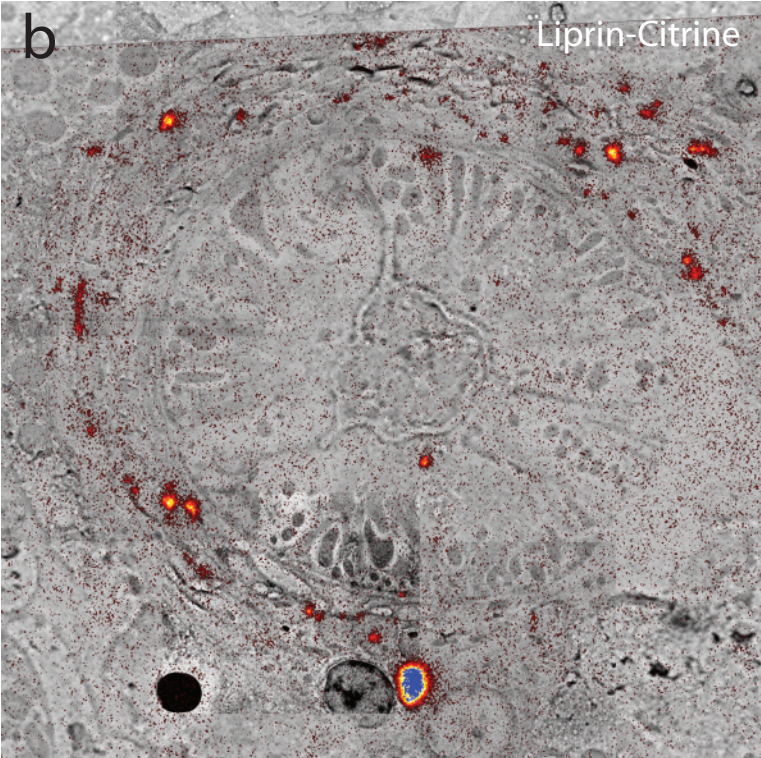
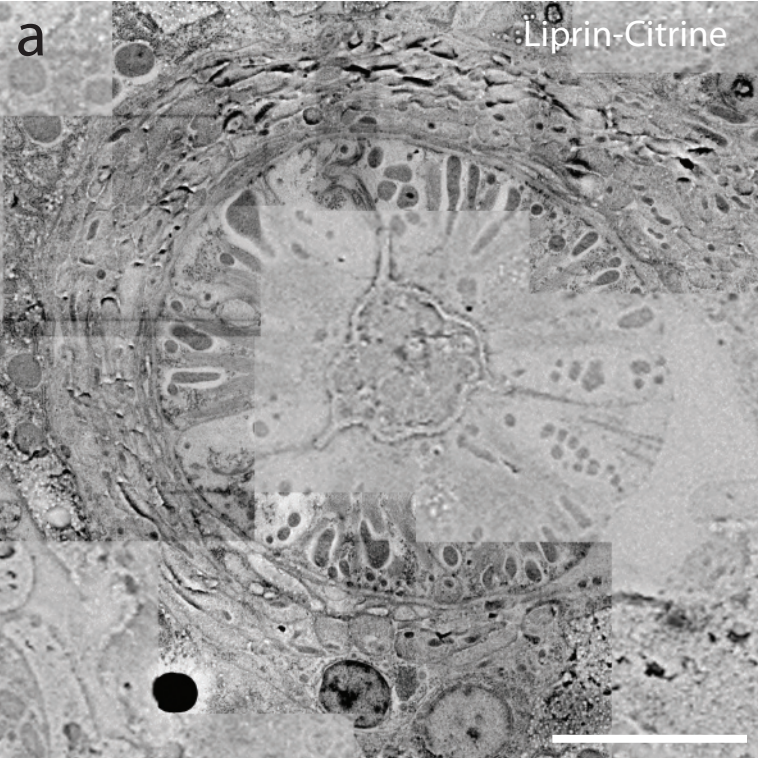


Supplementary Figure 1



Supplementary Figure 1: Preservation of morphology and fluorescence by different fixatives. **(a)** A TEM image of ventral nerve cord (VNC) fixed with 1% glutaraldehyde. **(b)** fluorescence micrograph of intestinal nuclei fixed with 1% glutaraldehyde. **(c)** A TEM image of VNC fixed with 0.1% osmium tetroxide. **(d)** A fluorescence micrograph of intestinal nuclei fixed with 0.1% osmium tetroxide. **(e)** A TEM image of ventral nerve cord (VNC) fixed with 0.1% potassium permanganate. **(f)** A fluorescence micrograph of intestinal nuclei fixed with 0.1% potassium permanganate preserves fluorescence well. **(g)** TEM image of the nerve ring fixed with 0.1% potassium permanganate + 0.001% osmium tetroxide. **(h)** A fluorescence micrograph of intestinal nuclei fixed with 0.1% potassium permanganate + 0.001% osmium tetroxide. Fluorescence images were acquired prior to plastic polymerization. Electron micrographs were acquired using a TEM. Transgenic animals (Citrine-Histone) were used to obtain the fluorescence images (**b**, **d**, **f**, and **h**) and electron micrographs of (**e**) and (**g**). Transgenic animals (*Pmyo-2::GFP*) were used to obtain electron micrographs of (**a**) and (**c**). The gain and exposure time of the camera were the same for (**b**, **f**, **h**), but for (**d**), the gain was increased 4x, and the exposure time was increased from 430 ms to 1000 ms to visualize the signal. Arrowheads indicate fluorescent signals in nuclei. In all images, resin was LR White with 5% water, pH 6.5. Black arrowheads indicate each synaptic vesicle in the electron micrographs. 'mito', mitochondria; 'dp', dense projection. Scale bars, 300 nm (**a**, **c**, **e**, **g**) and 30 μ m (**b**, **d**, **f**, **h**).

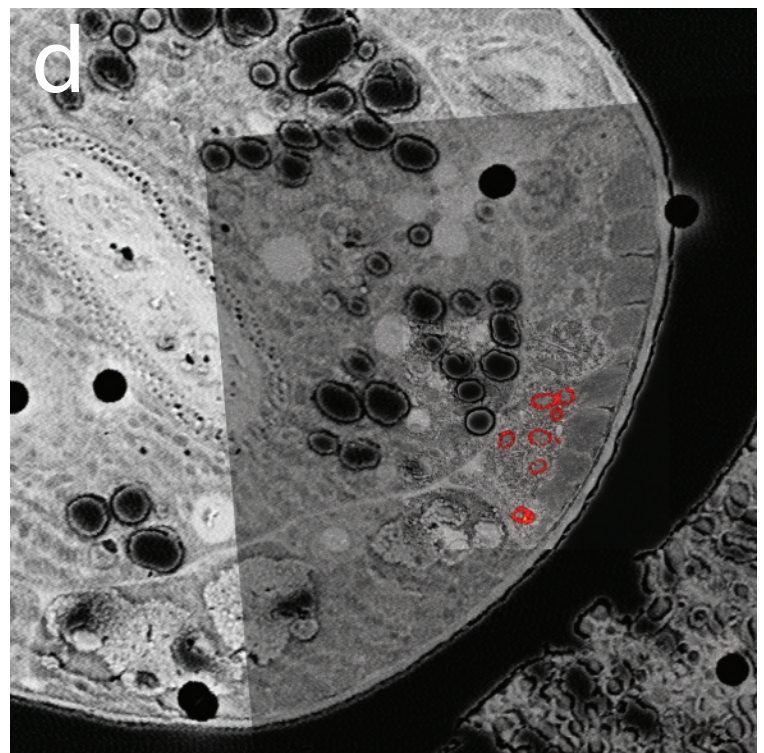
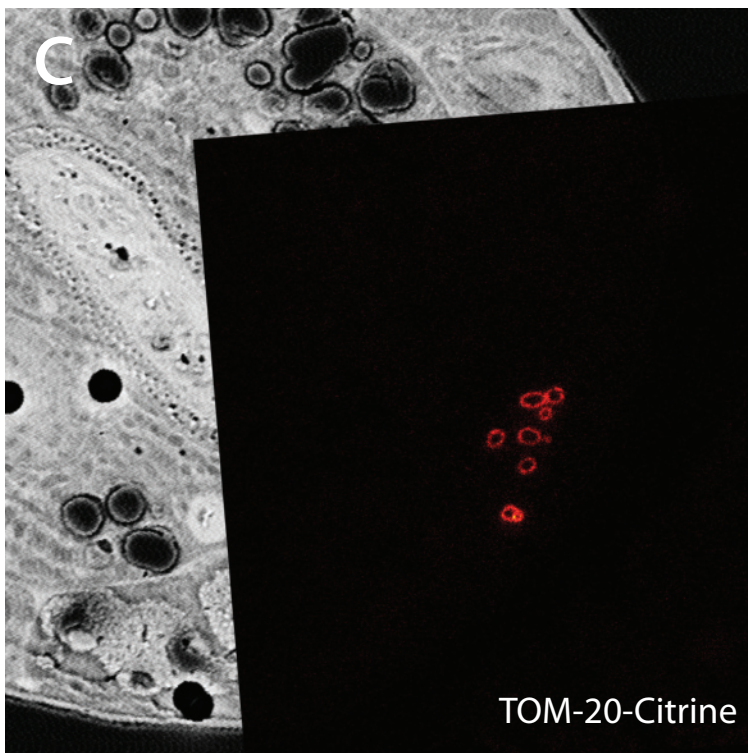
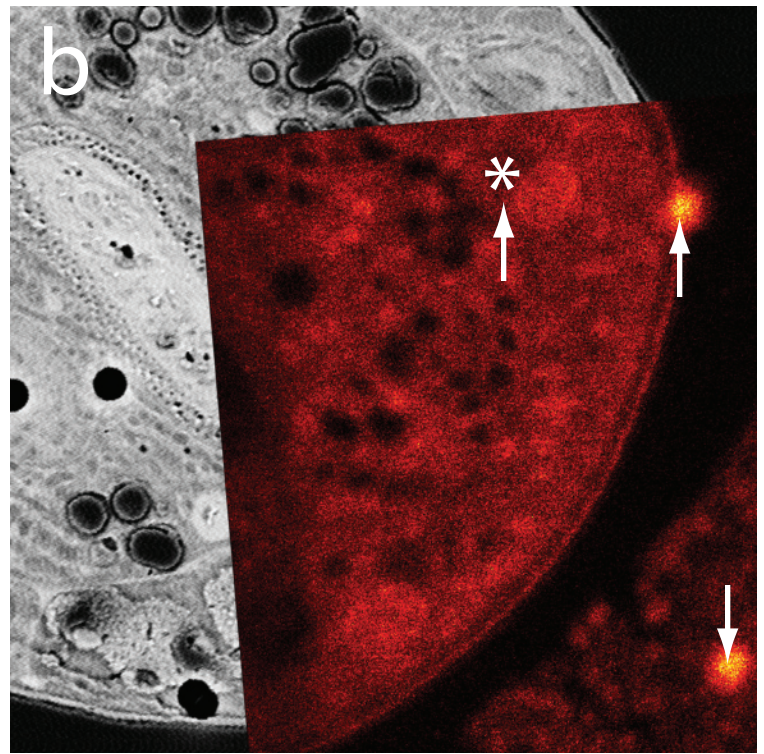
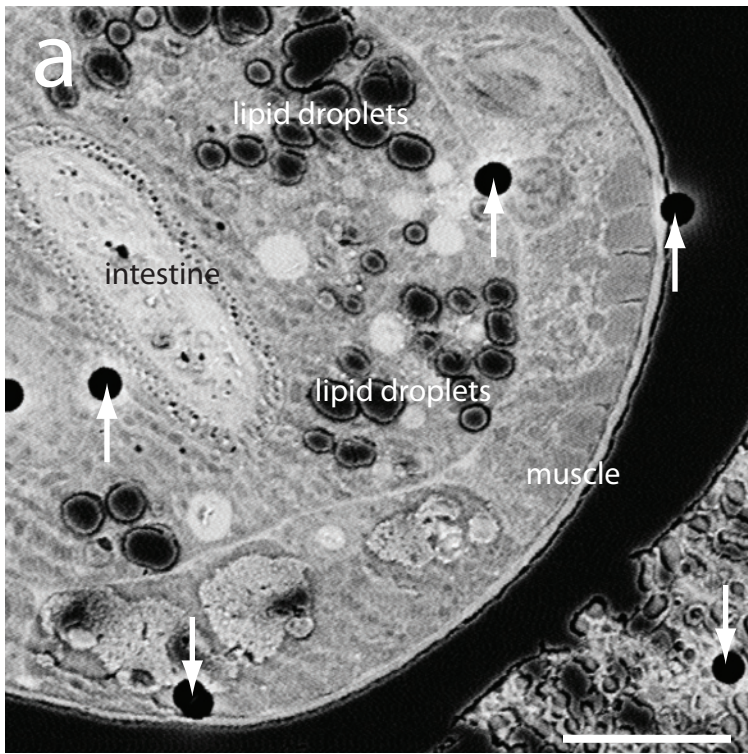
Supplementary Figure 2



Supplementary Figure 2: Liprin localization at low magnification. High magnification electron micrographs of neurons are tiled on top of low magnification micrographs to depict morphology and protein localization in the nerve ring and head ganglia.

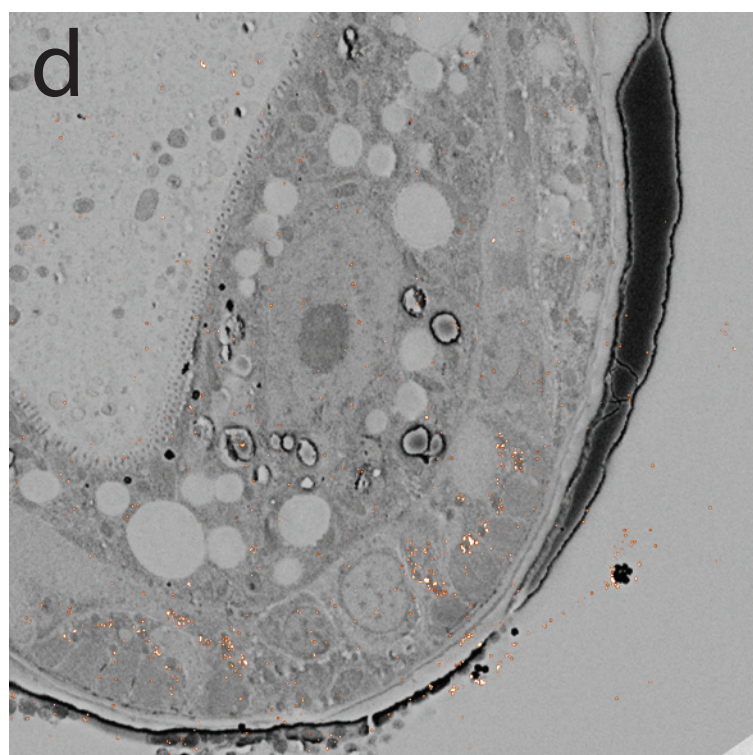
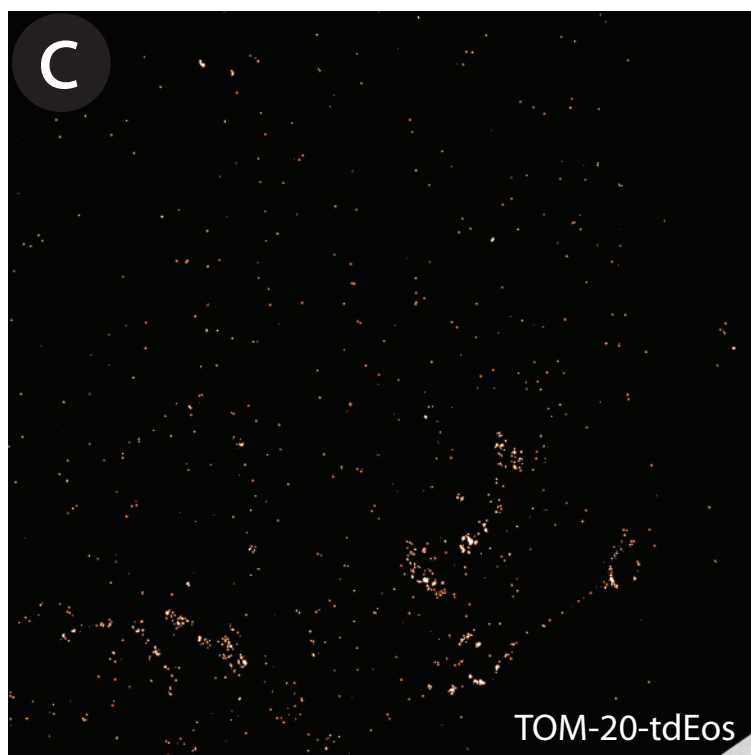
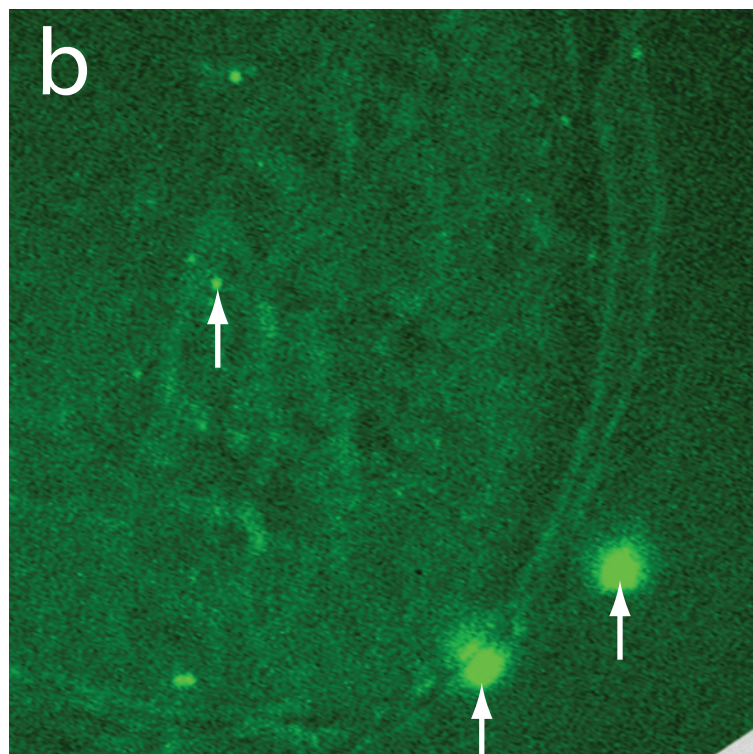
(a) Electron micrograph of nerve ring of a Liprin-Citrine expressing strain, **(b)** Correlative STED and electron micrograph of Liprin-Citrine. Note large aggregate of liprin adjacent to the nucleus of a neuron cell body at the bottom of the micrograph. **(c)** Electron micrograph of head ganglion. **(d)** Correlative PALM and electron micrograph of Liprin-Dendra. Note the aggregations of liprin in the cell bodies adjacent to the nuclei. Scale bars, 5 μm (**a-d**).

Supplementary Figure 3



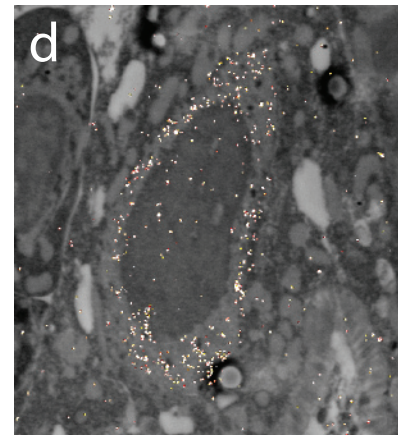
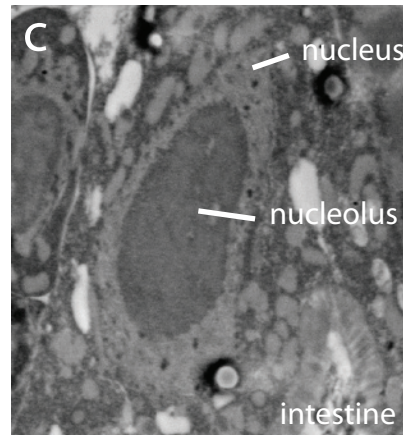
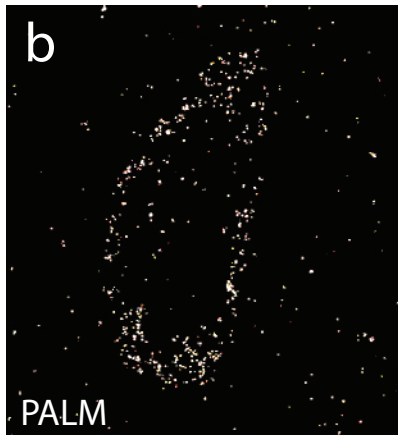
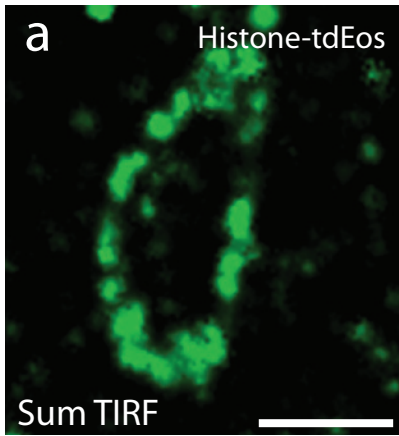
Supplementary Figure 3: Silica beads were used to align fluorescence and electron micrographs. **(a)** A low magnification electron micrograph (5000x) from a cross section of *C. elegans* expressing TOM-20-Citrine. Black circles, indicated by white arrowheads, are the fiduciary marks from silica beads applied prior to STED imaging. **(b)** An image of fiduciary markers is aligned onto an electron micrograph based on the location of the fiduciary marks. * indicates a silica bead that was not present during the STED recording. Presumably the bead moved during the post-staining with uranyl acetate just prior to SEM imaging. **(c)** The STED image is then rotated and translated based on the values obtained in **(b)**. **(d)** A gradient transparency is applied to the STED image so that the transparency of the background is reduced to 20% while that of citrine fluorescence remains at 100%. Scale bars, 5 μm **(a-d)**.

Supplementary Figure 4



Supplementary Figure 4: Gold nanoparticles were used to align fluorescence and electron micrographs. **(a)** A low magnification electron micrograph from a cross section of *C. elegans* expressing TOM-20::tdEos. Black dots are the fiduciary marks from 100 nm gold nanoparticles applied prior to PALM imaging. **(b)** An image of fiduciary markers is aligned onto an electron micrograph based on the location of the fiduciary marks. Note that the two bright spots on the lower right arise from clusters of gold particles. **(c)** A PALM image is then rotated and translated based on the values obtained in **(b)**. **(d)** A gradient transparency is applied to the PALM image so that the transparency of the background is reduced to 20% while that of tdEos fluorescence remains at 100%. Scale bars, 5 μm **(a-d)**.

Supplementary Figure 5



Supplementary Figure 5: Histone localization in an intestinal nucleus is similar by correlative PALM-EM to what was observed using correlative STED-EM. **(a)** Sum TIRF image of Histone-tdEos acquired from a thin section (70 nm). Sum TIRF image represents all the photons detected by the camera during the experimental time course. **(b)** Corresponding PALM image of Histone-tdEos. **(c)** Electron micrograph of an intestinal cell nucleus acquired from the same section. **(d)** Correlative PALM and electron microscopy of Histone-tdEos. The fluorescent signals are tightly localized to the nucleus. The sample was embedded in LR White. Scale bars, 3 μm (**a-d**).

Supplementary Table 1: Oligonucleotides

oGH55	GGGACAAGTTTGTACAAAAAAGCAGGCTTAAAAATGAGTAAAGGAGAAGAAGCTTTTCACT
oMPD6	GGGGACCACTTTGTACAAGAAAGCTGGGTATTTGTATAGTTCATCCATGCC
oGH95	GGGGACAAGTTTGTACAAAAAAGCAGGCTTCGCCACCATGAGTGCGATTA
EOS_rev	GGGGACCACTTTGTACAAGAAAGCTGGGTgTCGTCTGGCATTGTCAGGCAATC
oGH76	TCTTGTACAAAGTGGTGAGTAAAGGAGAAGAAGCTTTTCACTG
oGH57	TGGCGTCGATCATCCTTTGTATAGTTCATCCATGCC
oGH96	TCTTGTACAAAGTGGTCGCCACCATGAGTGCG
oGH94	TGGCGTCGATCATCCTGGCTGATTATGATCTAGAGTCGCG
oGH38	CCACTTTGTACAAGAAAGTTGAAC
oGH39	GGATGATCGACGCCAAC
oRJH19	GGGGACAAGTTTGTACAAAAAAGCAGGCTGTTATTCACTTTCTGCAAGGTATGAC
oRJH20	GGGGACCACTTTGTACAAGAAAGCTGGGTAGGTATATAAATGAAACTCGTAGGATTTTGC
oRJH21	tggagggatccATGAACACCCCGGAATTAACC
oRJH22	tgctaactagtGTTGGAATTCGAAGCTTGAGCTC
oRJH23	GGGGACAAGTTTGTATAGAAAAGTTGTTTCCTTCAGAAGACGTGCTTTCC
oRJH24	GGGGACTGCTTTTTTTGTACAAACTTGGGTGACTGAAAGTTTGATTG

Supplementary Note 1: Strains

The wild type is Bristol N2.

EG5582 *oxSi282*[*Phsp-16.41::Citrine::HIS-11::unc-54 3'UTR*] II; *unc-119(ed3)* III

EG5576 *oxSi283*[*Phsp-16.41::tdEos::HIS-11::unc-54 3'UTR*] II ; *unc-119(ed3)* III.

EG5515 *lin-15(n765ts)* X ; *oxEx1329* [*Pmyo-3::TOM-20(N-term)::Citrine::let-858 3'UTR lin-15(+)*] LITMUS 38i]

EG5998 *oxSi203* [*Pmyo-3::TOM-20(N-term)::tdEos::let-858 3'UTR unc-119(+)*] II ; *unc-119(ed3)* III

EG6190 *ttTi5605*; *unc-119*; *oxEx1490*[*Psnt-1::SYD-2::citrine; unc-119(+)* *lin-15(+)*]

EG6191 *ttTi4348*; *unc-119*; *oxEx1491*[*Psnt-1::SYD-2::Dendra2; unc-119(+)* *lin-15(+)*]

Supplementary Note 2: Choice of fluorescent proteins

For STED microscopy, fluorescent proteins must possess a high photostability. eYFP and Citrine have been shown to be well-suited for STED¹. We choose Citrine as the fluorophore for STED because the quantum yield is slightly higher, and the transgenes (Citrine-Histone, TOM-20-Citrine, and liprin-Citrine) were expressed well in *C. elegans* animals.

For PALM, the fluorescent protein must be capable of conversion from a fluorescence inhibited (inactivated) to a non-inhibited (activated) state. Here, we focused on photo-convertible rather than simply photo-activatable fluorescent proteins since the preservation of fluorescence can be visualized and assessed before photoconversion. For example, Dendra and EosFP emit green light before photo-conversion, and red light after photo-conversion.

We evaluated potential photo-convertible fluorescent proteins based on the following characteristics: appropriate expression pattern in *C. elegans*, high photo-conversion efficiency, and bright fluorescence after photo-conversion. We examined mOrange, Dendra, mEosFP, mEosFP2, and tdEos for reliable expression in *C. elegans*. Fusion of mEosFP2 to TOM-20 caused perinuclear aggregations of the fluorescence in muscle cells, suggesting that the tag was causing proteins to aggregate. mOrange, Dendra, mEosFP, and tdEos fusions to TOM-20 appeared to be expressed in the expected locations in the cell.

Genes for different fluorescent proteins were fused to the open reading frame for histone H2B under the control of the heatshock promoter. The constructs were inserted into the genome using *Mos1*-mediated single copy insertion (MosSCI)². Following a heat shock, the photo-conversion of each fluorophore was tested in whole animals by exposing them to 405 nm light (or 488 nm for mOrange³). Only mOrange was not detectably photo-converted. The transgenic strains expressing Dendra, mEosFP, or tdEos were fixed using 0.1% potassium permanganate and embedded in LR White. We prepared 100 nm slices from each and compared the photon intensity after the photo-conversion on a Zeiss PAL-M microscope.

Supplementary Note 3: Steps for sample preparation

The sample preparation for electron microscopy consists of six steps. Rapid freezing under high pressure immobilizes water molecules without generating ice crystals⁴. The vitreous water is then replaced by a fixative dissolved in organic solvents such as acetone. Fixation of rapidly frozen tissue can preserve morphology better than

conventional fixation in which cells are immersed in fixatives. Plastic resin is then infiltrated into the fixed and dehydrated tissues and polymerized into a plastic block. Finally, the hardened block is sliced into ultra-thin sections of 30-70 nm and mounted. Each of these steps could potentially quench fluorophores and had to be optimized.

Supplementary Note 4: Freezing and solvents

To determine if freezing under high pressure reduced fluorescence, we simply froze animals expressing GFP in the pharyngeal muscles (*Pmyo-2::GFP*) and thawed them to room temperature without any further treatment. The fluorescence level in the frozen animals was comparable to animals that were not frozen. By contrast, organic solvents quenched fluorescence. The same transgenic strain was frozen and processed through the freeze-substitution either with 100% acetone or 95% acetone plus 5% water in the absence of fixatives. The fluorescence in the animals treated with 100% acetone was completely quenched while there was no reduction in fluorescence in animals processed with 95% acetone, compared with non-treated animals. The presence of water at all steps was essential for the maintenance of fluorescence⁵. Each of the remaining steps also perturbs fluorescence significantly; to maintain fluorescence signals certain fluorescent proteins, fixatives and resins were required.

Supplementary Note 4: Components of each plastic

Lowicryl K4M is a combination of triethyleneglycol-di-methacrylate and benzoin-methyl-ether with acrylic and methacrylic esters.

LR Gold is consisted of 80% Polyhydroxy substituted bisphenol A dimethacrylate resin, 19.6% C12 methacrylate ester, and 0.4% dimethyl para toluidine.

LR White is consisted of 80% Polyhydroxy substituted bisphenol A dimethacrylate resin, 19.6% C12 methacrylate ester, and 0.9% benzoyl peroxide.

References for Supplementary Notes

1. Nägerl, U.V., Willig, K.I., Hein, B., Hell, S.W. & Bonhoeffer, T. Live-cell imaging of dendritic spines by STED microscopy. *Proc. Natl. Acad. Sci. U.S.A* **105**, 18982-18987 (2008).
2. Frøkjaer-Jensen, C. et al. Single-copy insertion of transgenes in *Caenorhabditis elegans*. *Nat. Genet* **40**, 1375-1383 (2008).
3. Kremers, G., Hazelwood, K.L., Murphy, C.S., Davidson, M.W. & Piston, D.W. Photoconversion in orange and red fluorescent proteins. *Nat Methods* **6**, 355-358 (2009).
4. McDonald, K. Cryopreparation methods for electron microscopy of selected model systems. *Methods Cell Biol* **79**, 23-56 (2007).
5. Micheva, K. & Smith, S. Array tomography: a new tool for imaging the molecular architecture and ultrastructure of neural circuits. *Neuron* **55**, 25-36 (2007).